The Cryosphere Discuss., 8, 3069–3115, 2014
www.the-cryosphere-discuss.net/8/3069/2014/
doi:10.5194/tcd-8-3069-2014

The Cryosphere Discussions
Open Access

Glacier area and length changes in Norway from repeat inventories

S. H. Winsvold[1], L. M. Andreassen[2], and C. Kienholz[3]

[1]Department of Geosciences, University of Oslo, P.O. Box 1047 Blindern, 0316 Oslo, Norway
[2]Section for Glaciers, Snow and Ice, Hydrology Department, Norwegian Water Resources and Energy Directorate, P.O. Box 5091 Majorstua, 0301 Oslo, Norway
[3]Geophysical Institute, University of Alaska Fairbanks, 903 Koyukuk Drive, Fairbanks, AK 99775-7320, USA

Received: 7 May 2014 – Accepted: 18 May 2014 – Published: 10 June 2014

Correspondence to: S. H. Winsvold (s.h.winsvold@geo.uio.no)

Published by Copernicus Publications on behalf of the European Geosciences Union.

Abstract

In this study, we assess glacier area and length changes in mainland Norway from repeat Landsat TM/ETM+ derived inventories and digitized topographic maps. The multitemporal glacier inventory consists of glacier outlines from within three time ranges: 1947 to 1985 (GI_{n50}), 1988 to 1997 (GI_{1990}), and 1999 to 2006 (GI_{2000}). For the northernmost regions, we include an additional inventory (GI_{1900}), based on historic maps surveyed between 1895 to 1907. Area and length changes are assessed per glacier unit, for 36 subregions, and for three main parts of Norway: southern, central and northern Norway. The results show a decrease of the glacierized area from 2994 km^2 in GI_{n50}, to 2668 km^2 in GI_{2000} (totally 2722 glacier units), corresponding to an area reduction of −326 km^2, or −11 % of the initial GI_{n50} area. This is equivalent to an average change rate of −11 $km^2\,a^{-1}$ over the past 30 years. The average length change for the full epoch (within GI_{n50} and GI_{2000}) is −240 m, corresponding to an average length change rate of −8 $m\,a^{-1}$. Overall, the comparison reveals both area and length reduction as a general pattern, even though some glaciers have advanced. The three northernmost glacier regions show the strongest retreat rates, whereas the central part of Norway shows the lowest change rates. Glacier area and length changes indicate that glaciers in maritime areas in southern Norway have retreated more than glaciers in the interior, and glaciers in the north have retreated more than southern glaciers. These observed spatial trends in glacier change are related to a combination of several geographical factors like glacier geometry and elevation, and other climatic aspects, such as continentality and the North Atlantic Oscillation.

1 Introduction

Glaciers are key indicators of climate change, and thus their monitoring is important (e.g. Lemke et al., 2007). Remote sensing techniques are ideal for measuring glaciers on a large scale, as they cover remote glacierized areas at relatively low effort. Optical images provided by the Landsat TM/ETM+, Terra ASTER or SPOT HRS have proven to be very efficient for mapping of glacier extents (e.g. Paul et al., 2002; Paul and Kääb, 2005; Paul et al., 2007; Bolch et al., 2010; Nuth et al., 2013). Glacier outlines are typically obtained from satellite images by using thresholded multispectral band ratios (Bayr et al., 1994; Sidjak and Wheate, 1999; Paul and Kääb, 2005; Kargel et al., 2014). An important advantage of the Landsat TM/ETM+ sensors is their large swath width, which is ideal for mapping vast glacier regions.

Glacier inventory data are used for modelling glacier mass balance (e.g. Marzeion et al., 2012; Radić and Hock, 2013), estimating ice volumes (e.g. Huss and Farinotti, 2012; Grinsted, 2013; Andreassen et al., 2014), or predicting global sea level rise (e.g.Leclercq et al., 2011; Gregory et al., 2013).

Despite Norway's long tradition of monitoring glaciers, there are still few data available on spatio-temporal change. Due to the favourable topography and climate in Norway, hydro-power accounts for 98 % of the electricity in Norway, and about 15 % of the run-off comes from watersheds that are partly glacierized (Andreassen et al., 2005). For this reason, the Norwegian Water Resources and Energy Directorate (NVE) maintains a database of glaciological data in mainland Norway. However, most of the glaciers have not been mapped due to remote locations. In addition, most glaciers in Norway lack information of the spatial and temporal variations of glacier change.

Previous glacier inventories of Norway from the 1960s to the 1980s lack digital glacier outlines (Østrem and Ziegler, 1969; Østrem et al., 1973, 1988), and glacier area and length assessments are not straight-forward to conduct using these data sets, e.g., due to unknown ice divides. The most recent satellite-derived glacier inventory of Norway is based on Landsat TM/ETM+ (Andreassen et al., 2012b). It uses a GIS-based approach, and is compiled following the Global Land Ice Measurements from Space (GLIMS) guidelines (Kargel et al., 2005; Racoviteanu et al., 2010). This data set is a highly detailed digital baseline product ideal for glacier area and length change assessments (Andreassen et al., 2008; Paul and Andreassen, 2009; Paul et al., 2011). Glacier length measurements are considered to be one of the most important ways to express glacier change in the future (Hoelzle et al., 2003). Historical data of length change observation can give much information about how glacier response to the climate (Leclercq et al., 2014). The newly compiled Norwegian glacier inventory is available through the GLIMS database, and as a published book (Andreassen et al., 2012b). Areas with multi-temporal glacier outline datasets are globally rare (Kargel et al., 2014). Because long term glacier change assessments are crucial for the understanding of glacier response to climate (Hoelzle et al., 2003), there is a need to complete such a multi-temporal glacier inventory.

For the first time, we present multi-temporal data sets derived from Landsat TM/ETM+ satellite images and topographic maps for all glacierized areas in Norway. We perform a glacier area and length change assessment which is based on three data sets within the time range of 1947 to 1985 (GI_{n50}), 1988 to 1997 (GI_{1990}) and 1999 to 2006 (GI_{2000}). We compare in situ length change observations with length changes from automatically derived centerlines. We extend the data sets prior to GI_{n50} using older topographic maps, which allows us to conduct an extended glacier area and length assessment on five ice caps in northern Norway. Concerning the multi-spectral band ratio technique, we demonstrate that mapped glacier areas are sensitive to small variations in the chosen thresholds.

2 Study region

Norway extends from 58 to 71° N, and from 5 to 31° E, and covers an area of 385 199 km^2 (0.7 % of the area) (Fig. 1a). The identified 2534 glaciers correspond to a glacierized area of 2692 ± 81 km^2 (using ±3 % as uncertainty) (Andreassen et al., 2012b). Divided into individual glacier units, the numbers of glacier units are 3143.

Coastal regions in Norway have a warm and moist maritime climate, while the interior is drier and colder. Climate gradients along a west–east transect are pronounced, especially in southern Norway. This west–east pattern is caused by the westerly winds and the Gulf Stream, together with the shading effect in the eastern parts due to the coastal mountains (Hanssen-Bauer et al., 2009). These climatic factors contribute to warmer conditions in Norway compared to similar latitudes elsewhere in the world. Norway has a latitudinal gradient in terms of temperature and precipitation, which both decrease from south to north. Although Norwegian glaciers span over ~ 1500 km from north to south, there is no pronounced variation in climate along the coast because of the ice-free Norwegian Sea (Fig. 1b). The mean equilibrium-line altitude (ELA) of the glaciers increases towards the inland, and decreases towards the north due to the climatic differences (Andreassen et al., 2005).

The first systematic glacier observations in Norway were initiated around 1900 (Hoel and Werenskiold, 1962), when glacier length change measurements started on several glaciers. Throughout the 20th century, the glaciers have generally retreated, except for intermittent advances of the coastal glaciers. Periods of increased winter precipitation have contributed to temporary mass gain on all glaciers. Advances were recorded around the years 1910 and 1930 and in the 1990s (Andreassen et al., 2005; Nesje et al., 2008). Although long time series of glacier measurements are available for selected glaciers, most glaciers were not monitored. Glacier inventories of Norway were published in 1973 for northern Norway (Østrem et al., 1973), and 1969 and 1988 for southern Norway (Østrem and Ziegler, 1969; Østrem et al., 1988). The first complete and satellite-remote sensing based inventory of Norway was published in 2012 (Andreassen et al., 2012b). In this paper, Norway refers to mainland Norway only. Area and length changes for Svalbard were recently published by Nuth et al. (2013).

3 Data and methods

3.1 Data set background

Our glacier inventory data are compiled using multi-spectral Landsat satellite data for the time periods GI_{2000} and GI_{1990}, topographic maps based on aerial photographs for GI_{n50}, and analogue maps to extend glacier outlines further back in time (GI_{1900}, prior to the GI_{n50} data set) (Fig. 2). In our analysis, we compare the datasets with each other resulting in three epochs: full epoch (GI_{n50}-GI_{2000}), epoch 1 (GI_{n50}-GI_{1990}) and epoch 2 (GI_{1990}-GI_{2000}).

In epoch 1 and epoch 2 some glaciers had less than 10 years between the two datasets compared, corresponding to 12 % of the numbers of glaciers in both GI_{1990} and GI_{2000} (Table 1). Ideally, glacier inventories should be retrieved in intervals of a few decades when used in change assessments, to account for the glacier response time (Haeberli, 2004). However, if a glacier region encounters very fast down-wasting of the glaciers, shorter mapping intervals can be used, which is the case for many Norwegian glaciers.

The multi-temporal data sets contribute to the monitoring of essential climate variables (ECVs), and follow the Global Climate Observing System principles (GCOS, 2003). The datasets were created in accordance with the guidelines on how to monitor glaciers and ice caps, established by the Global Terrestrial Network for Glaciers (GTN-G).

3.1.1 Division of glaciers

We divided the study area in three geographical parts: northern, central and southern Norway, which were further split into 36 subregions (map in Figs. 6 and 7). To create an inventory of individual units, glaciers were divided into glacier units based on ice divides. We used the Hydrology tools Flow accumulation and Flow direction in ArcGIS©. Flow accumulation creates a raster of accumulated flow into each cell, and Flow direction find the steepest down-slope neighbor for each cell. Both data sets are created from the national Digital Elevation Model (DEM, from the Norwegian Mapping Authority), and additionally discharge basins from NVE were used to define ice divides manually. In the GI_{1900}, GI_{n50} and GI_{1990}, each glacier complex was separated using the same ice divide as GI_{2000}. The glacier basins were adjusted to include glacier outlines from all three data sets. If GI_{1900}, GI_{n50} and GI_{1990} extended the GI_{2000} perimeter, e.g. due to disintegrating glaciers, the ice divides and glacier basins were adjusted using topology editing and the DEM. In GI_{2000} the 36 glaciers regions were arranged from north to south (map in Figs. 6 and 7), and within the regions glacier IDs (1–3143) were assigned automatically from north to south based on latitude. The Norwegian Glacier Inventory book includes maps and tables for all mapped glacier entities covered in GI_{2000} (Andreassen et al., 2012b).

3.2 GI_{2000} and GI_{1990} – Landsat satellite imagery

We used the Landsat TM/ETM+ satellite images rather than ASTER and SPOT due to the larger swath width of Landsat. The year of satellite acquisitions and the spatial coverage for the GI_{1990} and GI_{2000} data sets are presented in Fig. 2c and d. GI_{2000} and GI_{1990} span over a mapping period of 7 to 9 years respectively, as it proved impossible to map outlines for all Norwegian glaciers within one or a few years using Landsat TM/ETM+. This is due to lack of cloud-free Landsat TM/ETM+ satellite scenes, as a result of Norway's pronounced maritime climate. Seasonal snow cover, due to the high precipitation rates throughout all seasons, makes satellite image interpretation challenging (Andreassen et al., 2008). Due to extensive cloud coverage and partly also seasonal snow, full coverage for the GI_{1990} was not possible. No usable scenes were available for Jostedalsbreen, Lofoten/Hamarøy and a part of inner Troms (see Sect. 3.7).

Prior to the derivation of glacier outlines from the Landsat scenes, we carried out an accurate orthorectification and quality check of the images, using PCI Geomatica©. The Landsat L1T/L1G-products were delivered orthorectified, and often used as-is after a quality check (Table 2). However, selected satellite images had to be orthorectified prior to the derivation of outlines, due to insufficient quality on the L1T/L1G-products, especially in mountainous areas. The root mean square values (RMSE) for both the purchased satellite scenes and the orthorectified ones have an accuracy of less than ~ 30 m.

We calculated the band ratios for the Landsat images by including the red band (TM_3), and the short wave infrared band (TM_5). The band ratio method uses threshold values optimized for each satellite scene. We used $\frac{TM_3}{TM_5} \geq t_1$, where t_1 varied between 1.6 to 2.8. To improve results in shadowed areas, we included an additional threshold on the blue band, $TM_1 \geq t_2$, where t_2 is either 35 or 60, with some exceptions (Table 2) (Paul and Kääb, 2005; Paul and Andreassen, 2009). In addition, glacier outlines were manually corrected in case of debris cover, glacier–lake interfaces, clouds or glaciers in cast shadow which were not mapped automatically. Only very few outlines had to be corrected for debris cover since the glaciers in Norway are mostly debris free. Lakes and seasonal snow misclassified as glaciers were masked out from the glacier outline product. For the manual corrections and the delineations of ice divides, we used topology editing in ArcGIS©. Topology rules allowed features that share the same geometry to be updated simultaneously. The methods of human inspection and editing of the data sets are carefully described in the glacier inventory by Andreassen et al. (2012b).

3.2.1 Band ratio accuracy and threshold sensitivity

The accuracy of the band ratio method and the sensitivity of the used threshold values are essential for change assessment of glaciers. Orthophotos from the same acquisition year as the satellite images are ideal for determining the accuracy, but are rarely available. In Jotunheimen, a mountain region in southern Norway, glacier outlines were compared with orthophotos taken one year apart, and an area difference of −2.4 % was found (Andreassen et al., 2008). Similar results were found on a test site in the Swiss Alps, where outlines derived from Landsat TM imagery were compared with a SPOT satellite scene, which revealed an area difference of 2.3 % (Paul et al., 2002). For debris-free glaciers, the band ratio method is robust and accurate (Albert, 2002; Paul et al., 2003), with an accuracy between ±2–5 % (e.g. Paul et al., 2013). Here, we operate with an accuracy of ±3 %, implying that the inventory of Norwegian glaciers has a total accuracy of $2692 \pm 81\,km^2$ (Andreassen et al., 2012b) ($2668 \pm 80\,km^2$ for the glaciers included in GI_{2000}). The automatic band ratio method and manual digitizations give similar result, but the band ratio method often obtains a smaller glacier area as it tends to exclude some mixed pixels (Paul et al., 2013).

The mapped glacier area strongly depends on the chosen threshold value. The sensitivity of selected threshold values used on the ratio $\frac{TM_3}{TM_5} \geq t_1$ and the additional blue band $TM_1 \geq t_2$, have been investigated for 57 glacier units in western Finnmark, Northern Norway. A Landsat 5 TM satellite scene with good snow and cloud conditions from the year 2006 was used (Area code 1_{2000} in Table 2). By calculating the difference in number of pixels mapped for selected thresholds, a percentage difference of area relative to the applied threshold is calculated (Fig. 3). We used $\frac{TM_3}{TM_5} \geq 2.4$ and $TM_1 \geq 35$ or 60 as reference values (totally 69.3 and 65.6 km^2 respectively). The $\frac{TM_3}{TM_5}$ ratio thresholds range from 2.0 to 2.8 with increments of 0.2. There were some outliers strongly affecting the mean values of area change between the thresholds compared, thus it is more representative to use median values (Fig. 3a).

Using $\frac{TM_3}{TM_5} \geq 2.8$ to 2.4, and $TM_1 \geq 35$, we find a median decrease in area of −11 % (−3.1 km^2). Higher threshold values used for $\frac{TM_3}{TM_5}$ reduces noise, but includes less glacier area due to removal of mixed ice and terrain pixels. Similar results are found when $\frac{TM_3}{TM_5} \geq 2.0$ to 2.4, and $TM_1 \geq 35$ (median area increase of 12 %). This means a larger glacier area is mapped, also for glaciers in cast shadow, but it also implies that more noise was included in terms of mixed pixels. The $\frac{TM_3}{TM_5}$ should be as low as possible to include the dirty ice around the glacier perimeter (Paul et al., 2013). If $\frac{TM_3}{TM_5} \geq 2.4$ was used with $TM_1 \geq 60$ we find less variation of the area compared to the reference threshold value. A median area decrease of −4 % (−1.2 km^2) using $\frac{TM_3}{TM_5} \geq 2.8$ to 2.4, and median area increase of 3 % using $\frac{TM_3}{TM_5} \geq 2.0$ to 2.4.

By applying a threshold of $TM_1 \geq 35$, the area mapped was more sensitive and included more mixed pixels, compared to $TM_1 \geq 60$ (Fig. 3b and c). Glaciers in cast shadow are most sensitive to variations in the applied threshold, and manual on screen digitization was necessary in some occasions.

3.3 GI_{n50} – topographic maps

The GI_{n50} data set was derived by digitizing 168 first edition 1 : 50 000 topographical maps in the N50-series from the Norwegian Mapping Authority based on aerial photographs acquired between 1947 and 1985 (Fig. 2b). Otherwise, a comparison with previous glacier inventories would have been challenging due to different ice divides and the lack of digital outlines (Andreassen et al., 2008).

The first edition N50-paper maps were scanned and georeferenced using ground control points in a reference map (from European Datum zone 32, 33, and 34 to WGS 84 UTM zone 33). The glacier outlines were then digitized on-screen. We used first order polynomial transformation and obtained RMSE values of less than 10 m. The year of the aerial photographs were derived from information provided by the Norwegian Mapping Authority, but the acquisition year was also checked on every map sheet. Some map sheets (e.g. 1532-2 Altevatnet) have several acquisition years between 1947 and 1951 and thus, the exact acquisition year of the mapped areas is unknown. In those cases, the first mapping year (i.e. 1947) was allocated to the glaciers within the map sheet.

Three investigators digitized a sample of 10 glaciers in the Frostisen region, ranging from 0.06 to 0.93 km^2 by size (Frostisen map sheet 1331-2), to estimate the uncertainty arising from the subjective interpretation by the digitizer. 65 % of all glaciers in the GI_{n50} data set are within this size class, and are thus representative for many of the digitized glaciers. The standard deviations of the total glacier area were in the range from 0.0018 to 0.0066 km^2 for the 10 selected glaciers digitized by three different investigators. This indicates little variation in the digitizing accuracy between the interpreters, and minor effects on the end result.

A uncertainty analysis was not applied to the topographic maps, because of unknown working methods and mapping principles of the cartographers of the time.

3.4 GI_{1900} – analogue maps

The applicability of older analogue maps was tested in the two northernmost glacier regions in Norway (Seiland and Øksfjord, see Fig. 2a). A map series named *Gradteigskart* was used, which are quadrangle maps constructed from land surveys (map scale 1 : 100 000). The surveys of Seiland and Øksfjord were conducted in the period 1895–1907 (GI_{1900}), and cover three map sheets (174-92:1895, 174-106:1896 and 147-178:1907). The map sheets include the five largest ice caps in the two regions, Nordmannsjøkelen, Seilandsjøkelen, Øksfjordjøkelen, Svartfjelljøkelen and Langfjordjøkelen. The GI_{1900}-map sheets were scanned and georeferenced using local transformation methods. The glacier outlines were manually digitized from the georeferenced maps. Glacier outlines from the GI_{1900} data set are less accurate than GI_{n50}. Old analogue maps can have severe planimetric distortions due to complex topography, and in certain cases, glacier extents are known to be overestimated (Østrem and Haakensen, 1993). While it is worthwhile to incorporate these outlines into the change analysis, the results must be interpreted with care and considered as an estimate rather than an accurate benchmark.

For three composite glaciers in West-Finnmark (Langfjordjøkelen, Øksfjordjøkelen and Svartfjelljøkelen), we tested the spline, adjust, second order polynomial and third order polynomial transformation methods for the georeferencing. We used 25 ground control points in each map sheet, with a mean total RMSE of ±50 m. We chose to use the second order polynomial as transformation method, due to the best overlay with real topography and the other data sets. In total, the area of the second order polynomial transformation method was 89 km^2. Area differences between the tested methods varied up to 1.8 % (1.6 km^2) from the applied method.

3.5 Digital Elevation Model (DEM)

A DEM is required for deriving topographic parameters, ice divides and centerlines. We used GIS-analysis to extract glacier parameters from the data sets. Topographic

TCD
8, 3069–3115, 2014

parameters were calculated for GI_{2000}, including minimum, maximum, mean and median elevation, aspect, and slope. The spatial resolution of the DEM provided by the Norwegian Mapping Authority is 20 m, and the elevation contours, which the DEM was constructed from, were derived from aerial photography. We used one single DEM to calculate the topographic parameters for all our outlines. Accordingly, the date of the DEM is not always coincident with the date of the outlines. In case of GI_{2000}, the DEM data is up to ~20 years older than the outlines. Still, unless the elevation changes are very large, the surface changes have only a minor impact on many of the derived parameters, due to the extensive number of pixels averaged when calculating slope, mean altitude and aspect (Frey and Paul, 2012). However, minimum altitude is sensitive to the applied DEM, as the minimum elevation is highly affected by rapid changes in the glacier termini. Ideally, we would have had multi-temporal DEMs, with each outlines having its own DEM, but this is not available for our study area. Paul et al. (2011) explored the possibility to use the Advanced Spaceborne Thermal Emission and Reflection Radiometer global DEM (ASTER GDEM) in the Jostedalsbreen glacier region. The study revealed too many artifacts close to the termini of the glaciers, and concluded that the national DEM was a better choice. The DEM from the Norwegian Mapping Authority was used for all ice divides, except on Folgefonna and Hardangerjøkulen ice caps where DEMs based on LIDAR data achieved in 2007 and 2010 were adopted (Andreassen et al., 2012b).

3.6 Deriving centerlines

Glacier length is reported for all glacier units in the previous Norwegian glacier inventories (Østrem and Ziegler, 1969; Østrem et al., 1973, 1988). However, in the latest inventory of Norwegian glaciers, glacier length was not included (Andreassen et al., 2012b). In this study, we extend the inventory by adding glacier length.

We calculated centerlines by applying a three-step cost grid – a least cost route approach which requires glacier outlines and a DEM as input (Kienholz et al., 2014). We excluded the glaciers smaller than < 1 km^2 (from GI_{n50}) to reduce the noise from

TCD
8, 3069–3115, 2014
Glacier area and length changes in Norway
S. H. Winsvold et al.

the seasonal snow cover, which gives relatively larger errors over smaller areas. Our method for deriving centerlines was reproducible and fast, compared to digitizing flow lines by hand which can be very time consuming. In the first step, the algorithm identifies the lowest glacier points as termini, while using local elevation maxima along the glacier outlines to identify heads for each major glacier branch. In the second step, the algorithm determines the actual centerlines between heads and termini by calculating the least cost route on a cost grid (Fig. 4). The cost grid is established using the grid cells elevations and Euclidean distances to the glacier edge. To allow for plausible centerlines, the lowest cost values are allocated to the glacier center and to lower glacier reaches. In the third step, the algorithm divides the centerlines into individual branches, which are then classified according to a branch order (Kienholz et al., 2014). Each step of the algorithm is implemented independently, so that results can be checked visually and corrected if necessary.

For each glacier, the longest centerlines were extracted to describe glacier length, in agreement with previous studies (e.g. Paul et al., 2009). To calculate length change, we took the longest centerlines from the GI_{n50} dataset as a reference and clipped them with the more recent glacier outlines in the frontal areas (Fig. 4). We visually checked whether the clipped centerlines run through the glacier terminus in GI_{1900}, GI_{1990} and GI_{2000}. Edits were required in case of glacier advance, or perpendicular shift of the termini relative to the original centerline. In these cases, the centerlines were manually lengthened following contour lines. This was done for most of the datasets, and it was particularly important for the dataset GI_{1900} due to larger glacier areas than in GI_{n50}. The length change was calculated as the differences of the centerlines. Tests indicated that this procedure yielded more plausible length changes than recalculating the centerlines for each period, using the corresponding outlines. The main problem with such recalculating was that glacier recession often leads to the emergence of nunataks. The centerlines run around these new nunataks, increasing the glacier lengths, which interferes with the goal of isolating the change of the termini positions only.

In many cases the comparison between the centerlines from the glacier inventories was not doable, due to the fact that GI_{1900} did not always align with the other datasets, and the length change could not be measured. For instance, for Nordmannsjøkelen only 1 out of 9 glacier units could be used (Table 7).

Cumulative time series of glacier front position measurements were available from the database of NVE, and we compared these in situ length change measurements with our length changes derived from centerlines for the full epoch. We used data from 12 glaciers with corresponding measuring periods in both the in situ measurements by NVE and the cumulative length changes from topographic maps and satellite images derived in this study (Table 5). Additionally, five glaciers were compared for epoch 1, and six glaciers for epoch 2. Some of the measurements began after the GI_{n50} mapping year, but we choose to include series if the gap was not larger than 4 years. Using an uncertainty of ±1 pixel for satellite images, variations less than 30 m can not be expected to be identified (Paul et al., 2011).

3.7 Inclusion, exclusion and representation of data

Our objective is to include as much data as possible in our analysis, in order to provide the extensive presentation of the glacier variations in Norway. However, due to the heterogeneous nature of the data sets, we needed to exclude parts of the data for different analyses. From the GI_{n50} and GI_{1990} data sets, we include the glaciers that overlap in space with the GI_{2000}. We choose this approach, because the two earlier datasets tend to have higher uncertainties. For our analysis, we also included in total 400 snow fields or remnants of glaciers into the GI_{2000} glacier areas, to make a more precise analysis of the area change.

This results in a total of 2722 glacier units, an area of 2668 km^2, in the glacier area change (GAC) analysis for the full epoch, divided to 1396 glacier units in southern Norway, 666 glacier units in central Norway and 660 glacier units in northern Norway. For epoch 1 and 2, 1684 and 1953 glacier units were included in the analysis, respectively. In the glacier length analysis, we included 564 glaciers for the full epoch, 286 for epoch 1 and 283 for epoch 2. The reason for the significantly lower number of glaciers in the analyses for epoch 1 and 2 compared with the full epoch is insufficient satellite images due to the cloud cover and seasonal snow for the dataset GI_{1990} (see Sect. 3.2). Figure 2c presents the area where data were lacking for GI_{1990}. For example, during the Landsat TM 4/5 and ETM+ 7 operation period (1982–2012), the largest ice cap Jostedalsbreen in western Norway, where most of the data is missing, has only one Landsat satellite acquisition with preferable mapping conditions (from 16 September 2006). The mean area change for glaciers not overlapping in all epochs was $-0.119\,km^2$ (2722 glacier units), and when only including glaciers overlapping in all epochs mean area change was $-0.096\,km^2$ (1684 glacier units). The change in the mean area change value indicate that Jostedalsbreen and glaciers in western Norway have been retreating.

In many cases, change assessments were challenging due to adverse snow conditions in the GI_{n50} data set. A visual inspection of the terrain was done to discover entities characteristic for snow patches often accumulated in gullies and ridges. We used glacier basins to cut perennial and seasonal snow attached to the glaciers. Totally, 251 glacier units from the GI_{n50} data set were split using the glacier basins, and parts that were assumed to be seasonal snow ($119\,km^2$) were detached and removed. All in all, $396\,km^2$ was excluded from GI_{n50} data set including parts of glacier units and additional single snow patches. In GI_{1990} $64\,km^2$ was excluded outside the basins, and 183 glacier units were cut using the basins. However, the numbers are not comparable due to incomplete coverage of glaciers in the GI_{1990}-dataset.

4 Results and discussion

4.1 Glacier area changes

The glaciated area in mainland Norway has decreased from $2994\,km^2$ in GI_{n50}, to $2668\,km^2$ in GI_{2000}, corresponding to an area reduction of $-326\,km^2$. This means an average of $-11\,km^2\,a^{-1}$, during the full epoch (∼ 30 years), corresponding to a total reduction of −11 % (Table 3). Although most glaciers were subject to area loss, 20 % of the glaciers increased in area during the full epoch (in total 37 km^2). For epoch 1, 19 % of the glaciers increased in area, corresponding to 7.4 km^2. In epoch 2, 63 % of the glaciers gained area, corresponding to 98 km^2. Altogether for the three main parts, we find a clear decrease in glacier area for the full epoch (−10.9 %) as well as for epoch 1 (−10.5 %), but an increase in glacier area for epoch 2 (2 %). (Table 3). However, epoch 2 show an area gain for the northern (4.7 %) and central parts (8.3 %), whereas the southern region is decreasing in area (−7.1 %).

In Fig. 6, we present glacier area change for northern, central and southern parts and all the glacier regions and units of Norway for the full epoch using normalized values ($\frac{\mathrm{GAC}}{\mathrm{root}(A)}$ where A is the initial glacier area, Raup et al., 2009). This allows us to compare different groups with each other without exaggerating the influence of the small glaciers as is the case with values given in percentage or the large glaciers in the case of area changes given in absolute values (km^2) (Raup et al., 2009) (see Sect. 4.5). In Fig. 6b and c, we find less glacier area decrease, in the central part of Norway (glacier regions 13–19) for the full epoch. In the northernmost glacier regions 1–4, we find the strongest retreat pattern of the Norwegian glaciers (Fig. 6b). This is in line with in-situ observations from the only ice cap within monitoring program by NVE in this area, Langfjordjøkelen (Glacier region 2), which show a strongly negative mass balance and area reduction over the last few decades (Andreassen et al., 2012a). The negative trend of retreating glaciers has also been seen on Svalbard, north of mainland Norway. The area change of Svalbard glaciers show a total reduction of −7 % the last ∼ 30 years (Nuth et al., 2013).

Glaciers in northern Norway are located at lower elevations than glaciers in southern Norway, which may explain their stronger retreat seen over the epoch 1 and the full epoch (Fig. 6 and Table 3). The distribution of area with elevation is presented in Fig. 5 for northern and southern Norway for the GI_{n50} and GI_{2000} data sets, to demonstrate the glacier area change with elevation for the full epoch. Northern and central Norway are grouped because they show similar area-elevation distribution. For both southern and northern Norway we can see that the area decrease was larger at the lower elevations than on the high elevation glaciers of the groups, and area changes are observed at all elevations (Fig. 5). In the elevation range between 1000 to 1700 m a.s.l., corresponding to 62 % of the total elevation range, the total absolute area loss is 201 km^2 overall. Many of the largest ice caps in both southern and northern Norway are located in this elevation range, and there are only few glaciers above 1700 m a.s.l. in the central and northern Norway.

4.2 Glacier length changes

The total centerline length for all glaciers in the GI_{2000} data set (3143 glacier units) is 3282 km, the average length of the glaciers thus corresponds to 1 km. The average length change for the full epoch, is −240 m, corresponding to a retreat rate of 8 $m\,a^{-1}$ (Table 4). For comparison, we choose 286 glaciers that were included in all the data sets and whose area is > 1 km^2 in GI_{n50}. In this group of glaciers, the mean glacier centerline lengths are very similar between the two recent data sets, 2.86 km for GI_{2000} and 2.91 km for GI_{1990}, but the GI_{n50} has a longer mean glacier length of 3.11 km. The centerline data show that 11 % of the glaciers have advanced in the full epoch (average 88 m), and 5 and 30 % glaciers advanced in epoch 1 and 2, respectively. Glacier length changes show strong glacier retreat in all epochs and glacier regions, except for glacier region 19 in the full epoch (Fig. 7b). Overall, the length changes derived in this study show a steady retreat for many of the individual glacier units even though some have advanced (Fig. 7c). It should be emphasized that different number of glaciers were compared in the glacier area change and glacier length change assessment because there are significantly less data of the glacier lengths than areas (see Sect. 3.7). This may explain the different patterns of change for epoch 2 (Figs. 6 and 7). Overall, length changes for the three parts in Norway show a retreat of the glaciers for three epochs (Table 4).

TCD
8, 3069–3115, 2014

4.2.1 Glacier length changes vs. in situ length changes

Comparison of our glacier length changes with cumulative field data from NVE for 12 selected glaciers show mean deviation of 89 m (< 4 %) for the full epoch (Table 5), which indicates that the satellite and map derived glacier length changes are satisfying for groups of glaciers although the for individual glaciers the deviation can be relatively large. Nine of the glaciers show good agreement between the length change methods, corresponding to ±1 to 2 pixels.

The field measurements reveal that the rate of recession was variable and even absent for some glaciers, varying between −950 m (Fåbergstølsbreen in southern Norway, glacier ID 2289) to +149 m (Engabreen in northern Norway, Glacier ID 1094). Two of the glaciers compared show a deviation of more than 4 pixels (> 120 m). These glaciers are Fåbergstølsbreen and Stigaholtbreen. The discrepancy between the methods is most likely caused by error in some of the years of the in situ observations (Personal communication with Hallgeir Elvehøy (NVE), Desember 2013). For all the methods, the local topography in front of the glacier snout can affect the glacier length measurements. Additionally, changes of the glacier terminus do also change the morphology in front of the glacier, and makes it difficult to compare the measurements (Winkler et al., 2009). A limitation of using satellite images is the determination of glacier terminus in cast shadow, causing uncertainties in the derived length change (Paul et al., 2011). In our case, Fåbergstølsbreen (Glacier ID 2289) was actually located in cast shadow at the time of acquisition. The deviation can also be caused by differences in the measurement angle of the interpreter on the ground from a reference point toward the glacier, and the path of the centerline used to derive length change from glacier outlines.

4.3 Glacier change since the beginning of 1900s

Using analogue maps from the beginning of the 1900s (GI_{1900}), we extended the glacier area and length change assessment further back in time for five ice caps or former ice caps (Fig. 8). Similar methods and data sets have been used for detecting a century of glacier retreat on Kilimanjaro (Cullen et al., 2013). From these five ice caps, a total of 57 glaciers were included in this glacier area change analysis, and 26 centerlines were used for the glacier length change analysis here (Table 7). One of the challenges deriving glacier change in this region was disintegrating glaciers, in particular Nordmannsjøkelen (Fig. 8). The glacier geometry was changing extensively especially when it comes to emerging rock outcrops and ice patches separated from their tributaries. The glaciers response to the climate was not changes in the glacier dynamics, but rather by down-wasting (Paul et al., 2004).

Totally, the five ice caps have retreated from 139 to 65 km^2 from the 1900s to 2006 (Fig. 8). The mean area change from GI_{1900} to GI_{2000} (whole period) for the five ice caps is 1.3 km^2 (53 % in total), and the glacier length measurements show a mean retreat of 1063 m (37 % in total) (Table 7). The mean decadal change for both area and length show highest retreat rates for epoch 0 between GI_{1900} and GI_{n50} with -0.13 km^2 (length change of -73 m), where epoch 1 and 2 show retreat rates of -0.04 km^2 (length change of -35 m) and -0.03 km^2 (length change of -42 m), respectively (Table 6). Thus, these glaciers have been disintegrating and down-wasting extensively since 1900.

4.4 Spatial and temporal variation of glacier changes

4.4.1 Climate anomalies during the 20th century

Our results show that glaciers in Norway have been receding through the last ~30 years. This has also been seen in the in-situ data of individual glaciers (Andreassen et al., 2005, 2011). These data also show the maritime glaciers have been oscillating between periods of advance and recession, with recession being the most frequent state (Andreassen et al., 2005). The strong reduction in area and length in epoch 0 (GI_{1900} to GI_{n50}, Table 6) includes the warm period starting from the 1930s (Hanssen-Bauer, 2005) and causing severe glacier retreat (Østrem and Haakensen, 1993; Andreassen et al., 2005, 2008).

Transient mass surplus resulting from increased snow accumulation in the 1990s caused an advance, which is reflected in epoch 2 for both northern and central Norway (Fig. 6a, and see Sect. 4.1), as an increase in glacier area (Table 3). The 1990 advance that our results demonstrate, was most likely retained in the GI_{2000} data set in terms of some snow around the glacier perimeters and mass gain, especially in maritime areas. Many of the maritime glaciers have high mass turnover and thus are more sensitive to changes in precipitation rather than temperature (Oerlemans and Reichert, 2000). Glacier variations do not only respond to temperature changes during the ablation-season, but are also highly related to the amount of precipitation in the accumulation-season (Nesje, 2005). For several outlet glaciers from Jostedalsbreen a terminus response time of 3–4 years was observed between the mass gain and the related length change during the 1990s (Winkler et al., 2009).

4.4.2 Elevation

We did not find significant relationship between slope and glacier length or area change for our data sets, although the data show a trend for less glacier change with increasing slope, as previously shown by (Leclercq et al., 2014). Our results show that ice caps in northern Norway are particularly vulnerable to glacier area and length changes, because they are located in a maritime climate and at lower elevations compared with many of the ice caps in southern Norway (Figs. 5 and 8). Since the beginning of the 2000s all glaciers monitored by NVE have been in a state of retreat (Andreassen et al., 2005; Winkler et al., 2009). These strong changes are partly attributable to the glacier geometries: ice caps in Norway have a high fraction of their surface close to the modern equilibrium line, which makes them highly sensitive to climate changes (e.g., Nesje et al., 2008). For a steep glacier the main part of the accumulation area is situated in the highest part, and the sensitivity is lower. However, if the main part of the accumulation area is close to the ELA then the sensitivity is higher. If the equilibrium line rises, large parts of the accumulation area is transferred to the ablation area, and the mass balance becomes strongly negative. The accumulation-area ratio (AAR) for Langfjordjøkelen in

TCD
8, 3069–3115, 2014

the northernmost region, have shown to be 0 % for many years during the 2000s, and the glacier is far from being adapted to the present climate conditions (Andreassen et al., 2012a).

4.4.3 Climatic transects

We have inspected how glacier area and length changes are distributed in terms of a west–east transect in our data sets. The west–east transect reaches from Ålfotbreen in the west, to Gråsubreen in the east (Fig. 9a). Figure 9b illustrates yearly glacier area changes in a west–east transect for the full epoch. The annual glacier length change for the full epoch shows similar change pattern as the area change (Fig. 9c). Even though most of the glaciers have a large spread, the figure shows that the area changes and length changes are consistently lower for maritime glaciers, compared to the continental glaciers. The glaciers located in the precipitation “shadow” of the mountains in the east have less variation in glacier area and length change (Fig. 9). The mean winter balance on Gråsubreen is about 0.8 m water equivalent (w.e.), only ∼ 20 % of the winter balance on Ålfotbreen (3.7 m w.e.) (Andreassen et al., 2005). Representing glacier area changes along a climatic transect, illustrates the regional variation of glacier response to climate (Paul et al., 2007). Due to global warming glacier retreat will continue, and glaciers located in a maritime climate are expected to be more sensitive compared to glaciers located in continental areas (Hoelzle et al., 2003). Maritime glaciers have a high mass balance gradient compared to continental glaciers, which implies that glaciers located at the coast will respond faster to a changing climate. The drier continental glaciers are very dependent on the summer temperatures, and for maritime glaciers the spring/fall temperatures are important for the glacier sensitivity (Oerlemans and Reichert, 2000).

Our results of glacier area and length changes in the northernmost glaciers, shows the highest change signal in terms of retreat in Norway (Figs. 6 and 7 and Tables 3 and 4). Glaciers in Norway span over a transect of ∼ 1500 km from south to north. Much of the annual variation in Norwegian climate can be described by the North Atlantic

TCD
8, 3069–3115, 2014

Oscillation (NAO) index (Hurrell, 1995). The NAO influences the winter and annual surface mass balance, but its effect is reduced towards more continental glaciers (Nesje et al., 2000), as well as glaciers in higher latitudes. Langfjordjøkelen, the northernmost glacier with surface mass balance measurements, does not show as strong correlation with NAO as the other measured glaciers in Norway (Rasmussen, 2007), indicating glaciers located on higher latitudes are less affected by NAO. The latitudinal effect of solar radiation to the melt energy on Langfjordjøkelen in northern Norway plays a minor role compared with two glaciers in southern Norway, although the cloud cover is measured to be thicker at Langfjordjøkelen, which have a large effect on the surface energy fluxes (Giesen et al., 2014). Latitude has little influence on the glacier change signal, and the main reason for the highest retreat rates in northern Norway is the low glacier elevation and the higher ELA causing lowering of the accumulation-area ratio (Andreassen et al., 2012a).

4.5 Alternative ways to represent glacier area change

In this paper, we present our data of glacier area changes as absolute (km^2), relative (%) and normalized values for different time periods in order to provide a thorough presentation of the data. These methods give different representation of the change. For example, if a small glacier and a large glacier lose the same amount of mass with equal energy inputs, the percent change will be very different between the two. The small glacier will be overestimated in terms of change signal when compared with the large glacier, and we can say that the change signal of the small glacier is enhanced (Fig. 10b). When glacier change is expressed in terms of km^2-change, the opposite happens. A large glacier losing the same area in terms of km^2 as a small glacier with the same energy input, will be overestimated in terms of the change signal, and the signal of small glaciers can be lost (Fig. 10a). Our solution for this was to express glacier area change in a length scale dimension, called units of length. This can be done by normalizing by the square root of the initial area, $\frac{\mathrm{GAC}}{\mathrm{root}(A)}$, where GAC is glacier area change and A is the initial glacier area which is the $\mathrm{GI}_{\mathrm{n50}}$ when representing change

TCD
8, 3069–3115, 2014

for the full epoch (Raup et al., 2009). With this normalization, we removed the systematic trend that depends on initial glacier size (Fig. 10c). Additionally, by comparing this change signal with glacier length change measurements derived from glacier centerlines, one obtains a similar distribution of the two change signals (Fig. 10d).

Other alternative normalization strategies that also aim at expressing glacier area change in terms of units of length are possible, such as glacier area change over perimeter or glacier area change over width (personal communication with C. Nuth, May 2013). However, it is important to note that, for Norwegian glaciers, many different glacier types are present, with a variety of sizes and geometries. The "Box-method" uses the lower part of the glacier tongue for extracting glacier length change (Moon and Joughin, 2008; Nuth et al., 2013). This method was developed for marine-terminating glaciers, and is not an ideal method to use on many Norwegian glaciers, because of the many ice caps and cirque glaciers with often less distinctive glacier terminus.

5 Conclusions

We present a glacier area and length change analysis including multi-temporal data sets covering a larger area and higher temporal resolution than earlier studies. The glaciated areas in Norway are mapped from three glacier inventories within the period 1947 and 2006. Glacier area in mainland Norway decreased in all $-326\,\text{km}^2$ from GI_{n50} to GI_{2000}, corresponding to $-11\,\%$ during the last ~ 30 years. This corresponds to a yearly average area reduction of $-11\,\text{km}^2\,\text{a}^{-1}$. The average glacier length change for the last ~ 30 years has been $-240\,\text{m}$, which means an average yearly change of $-8\,\text{m}\,\text{a}^{-1}$. Glacier area and length changes indicate that glaciers in western Norway have retreated more than in eastern parts, and glaciers in the north have retreated more than southern glaciers. A combination of several factors like glacier geometry and elevation, climatic aspects such as continentality and the North Atlantic Oscillation, are related to the observed spatial trends in the glacier change analysis.

TCD
8, 3069–3115, 2014

The change assessment based on historical maps going back to beginning of 1900s in West-Finnmark reveal a very large reduction in glacier area from a total of 139 to 65 km^2, and a mean area and length change from GI_{1900} to GI_{2000} of −53 and −37 %, respectively.

Glacier outlines derived from topographic and historical maps have considerable uncertainties, due to challenges related to the seasonal snow cover by the time of mapping. Therefore, the results show the upper bound of glacier changes in Norway. The results differ regionally, but clearly exhibit a main trend of retreating glaciers during the last 30 years, even though some individual glacier entities have advanced.

The increased availability of automatically derived centerlines, makes it easier to retrieve glacier length changes when multi-temporal glacier inventory data are available, and it is reproducible. Glacier length change derived from centerlines, might be a more correct way to express glacier change signals due to the less dependency on glacier geometries. Sensors with higher spatial and temporal resolution (e.g. the Sentinel-2 satellite) opens new possibilities for observing glaciers in the future.

Author Contribution

The design and data for the three inventories were made by L. M. Andreassen and S. H. Winsvold. L. M. Andreassen and S. H. Winsvold developed the concepts of the study. C. Kienholz processed the centerlines for the multi-temporal dataset. S. H. Winsvold prepared the final data and wrote the original manuscript with contribution from L. M. Andreassen.

SVALI. This publication is contribution number 43 of the Nordic Centre of Excellence SVALI, “Stability and Variations of Arctic Land Ice”, funded by the Nordic Top-level Research Initiative (TRI).

Acknowledgements. The study was supported by a PRODEX project by the European Space Agency (ESA) called CryoClim, supported by the Norwegian Space Agency. The study is also a part of the SVALI project, and are also founded partly from here. Thanks to A. Kääb for guidance and suggestions to the work. The e-mail correspondence with Bruce Raup (NSIDC) has been appreciated in the discussion on how to represent glacier area change in a descriptive way. Thanks to C. Nuth (UIO) for input and feedbacks on the change analysis in general. Thanks to A. Voksø (NVE) for the design of the geodatabases and rules for topology editing of glacier outlines. Thanks to S. Engh for the manual digitization of the glacier outlines from the topographical maps in his summer job at NVE 2012. Thanks to all colleagues at UIO and NVE for fruitful discussions.

References

Albert, T. H.: Evaluation of remote sensing techniques for ice-area classification applied to the Tropical Quelccaya Ice Cap, Peru, Polar Geography, 26, 210–226, 2002. 3076

Andreassen, L., Elvehøy, H., Jackson, M., Kjøllmoen, B., and Giesen, R. H.: Glaciological investigations in Norway in 2010, NVE report 3, 2011. 3087

Andreassen, L. M., Elvehøy, H., Kjøllmoen, B., Engeset, R. V., and Haakensen, N.: Glacier mass-balance and length variation in Norway, Ann. Glaciol., 42, 317–325, 2005. 3071, 3073, 3087, 3088, 3089

Andreassen, L. M., Paul, F., Kääb, A., and Hausberg, J. E.: Landsat-derived glacier inventory for Jotunheimen, Norway, and deduced glacier changes since the 1930s, The Cryosphere, 2, 131–145, doi:10.5194/tc-2-131-2008, 2008. 3071, 3075, 3076, 3078, 3087, 3100

Andreassen, L. M., Kjøllmoen, B., Rasmussen, A., Melvold, K., and Nordli, Ø.: Langfjordjøkelen, a rapidly shrinking glacier in northern Norway, J. Glaciol., 58, 581–593, 2012a. 3084, 3089, 3090

Andreassen, L. M., Winsvold, S. H., Paul, F., and Hausberg, J. E.: Inventory of Norwegian Glaciers, NVE report 38, 2012b. 3071, 3072, 3073, 3075, 3076, 3080, 3103, 3110, 3111, 3112

Andreassen, L. M., Huss, M., Melvold, K., Elvehøy, H., and Winsvold, S. H.: Ice thickness measurements and volume estimates for glaciers in Norway, in preparation, 2014. 3071

Bayr, K. J., Hall, D. K., and Kovalick, W. M.: Observations on glaciers in the eastern Austrian Alps using satellite data, Int. J. Remote Sens., 15, 1733–1742, 1994. 3071

Bolch, T., Menounos, B., and Wheate, R.: Landsat-based inventory of glaciers in western Canada, 1985–2005, Remote Sens. Environ., 114, 127–137, 2010. 3071

Cullen, N. J., Sirguey, P., Mölg, T., Kaser, G., Winkler, M., and Fitzsimons, S. J.: A century of ice retreat on Kilimanjaro: the mapping reloaded, The Cryosphere, 7, 419–431, doi:10.5194/tc-7-419-2013, 2013. 3087

Frey, H. and Paul, F.: On the suitability of the SRTM DEM and ASTER GDEM for the compilation of topographic parameters in glacier inventories, Int. J. Appl. Earth Obs., 18, 480–490, 2012. 3080

GCOS: The Second Report on the Adequacy of the Global Observing Systems for Climate in Support of the UNFCCC, GCOS-82, World Meteorological Organisation, Geneva (WMO/TD No.1143), available at: http://www.wmo.int/pages/prog/gcos/Publications/gcos-82_2AR.pdf (last access: 5 June 2014), 2003 3074

Giesen, R. H., Andreassen, L. M., Oerlemans, J., and Van den Broeke, M. R.: Surface energy balance in the ablation zone of Langfjordjøkelen, an arctic, maritime glacier in northern Norway, J. Glaciol., 60, 57–70, 2014. 3090

Gregory, J. M., White, N. J., Church, J. A., Bierkens, M. F. P., Box, J. E., van den Broeke, M. R., Cogley, J. G., Fettweis, X., Hanna, E., Huybrechts, P., Konikow, L. F., Leclercq, P. W., Marzeion, B., Oerlemans, J., Tamisiea, M. E., Wada, Y., Wake, L. M., and van de Wal, R. S. W.: Twentieth-century global-mean sea level rise: is the whole greater than the sum of the parts?, J. Climate, 26, 295–306, 2013. 3071

Grinsted, A.: An estimate of global glacier volume, The Cryosphere, 7, 141–151, doi:10.5194/tc-7-141-2013, 2013. 3071

Haeberli, W.: Glaciers and ice caps: historical background and strategies of worldwide monitoring, in: Mass Balance of the Cryosphere – Observations and Modelling of Contemporary and Future Changes, edited by: Bamber, J. L. and Payne, A. J., Cambridge University Press, Cambridge, 559–578, 2004. 3074

Hanssen-Bauer, I.: Regional temperature and precipitation series for Norway: analyses of time series updated to 2004, Met.no, Rep. 15/2005, 34 pp., 2005. 3087

Hanssen-Bauer, I., Drange, H., Førland, E. J., Roald, L. A., Børsheim, K. Y., Hisdal, H., Lawrence, D., Nesje, A., Sandven, S., Sorteberg, A., Sundby, S., Vasskog, K., and Ådlandsvik, B.: Klima i Norge 2100, Bakgrunnsmateriale til NOU Klimatilplassing, Norsk klimasenter, september, 148 pp., 2009. 3073

Hoel, A. and Werenskiold, W.: Glaciers and snowfields in Norway, Norsk Polarinstitutt Skrifter, Oslo, Norway, 114, 1962. 3073

Hoelzle, M., Haeberli, W., Dischl, M., and Peschke, W.: Secular glacier mass balances derived from cumulative glacier length changes, Global Planet. Change, 36, 295–306, 2003. 3072, 3089

Hurrell, J.: Decadal trends in the North Atlantic oscillation, Science, 269, 676–679, doi:10.1126/science.269.5224.676, 1995. 3090

Huss, M. and Farinotti, D.: Distributed ice thickness and volume of all glaciers around the globe, J. Geophys. Res.-Earth, 117, F04010, doi:10.1029/2012JF002523, 2012. 3071

Kargel, J. S., Abrams, M. J., Bishop, M. P., Bush, A., Hamilton, G., Jiskoot, H., Kääb, A., Kieffer, H. H., Lee, E. M., Paul, F., Rau, F., Raup, B., Shroder, J. F., Soltesz, D., Stainforth, D., Stearns, L., and Wessels, R.: Multispectral imaging contributions to global land ice measurements from space, Remote Sens. Environ., 99, 187–219, 2005. 3071

Kargel, J. S., Leonard, G. J., Bishop, M. P., Kääb, A., and Raup, B.: Global Land Ice Measurements from Space, Series: Geophysical Sciences, Springer-Verlag, Berlin, Heidelberg, 810 pp., 2014. 3071, 3072

Kienholz, C., Rich, J. L., Arendt, A. A., and Hock, R.: A new method for deriving glacier centerlines applied to glaciers in Alaska and northwest Canada, The Cryosphere, 8, 503–519, doi:10.5194/tc-8-503-2014, 2014. 3080, 3081

Leclercq, P. W., Oerlemans, J., and Cogley, J. G.: Estimating the glacier contribution to sea-level rise for the period 1800–2005, Surv. Geophys., 32, 519–535, 2011. 3071

Leclercq, P. W., Oerlemans, J., Basagic, H. J., Bushueva, I., Cook, A. J., and Le Bris, R.: A data set of worldwide glacier length fluctuations, The Cryosphere, 8, 659–672, doi:10.5194/tc-8-659-2014, 2014. 3072, 3088

Lemke, P., J. Ren, R.B. Alley, I. Allison, J. Carrasco, G. Flato, Y. Fujii, G. Kaser, P. Mote, R.H. Thomas and T. Zhang: Observations: Changes in Snow, Ice and Frozen Ground, in: Climate Change 2007: The Physical Science Basis. Contribution of Working Group I to the Fourth Assessment Report of the Intergovernmental Panel on Climate Change, edited by: Solomon, S., Qin, D., Manning, M., Chen, Z., Marquis, M., Averyt, K. B., Tignor, M., and Miller, H. L., Cambridge University Press, Cambridge, United Kingdom and New York, NY, USA, http://www.ipcc.ch/publications_and_data/ar4/wg1/en/ch4.html (last access: 5 June 2014), 2007. 3070

Marzeion, B., Jarosch, A. H., and Hofer, M.: Past and future sea-level change from the surface mass balance of glaciers, The Cryosphere, 6, 1295–1322, doi:10.5194/tc-6-1295-2012, 2012. 3071

Moon, T. and Joughin, I.: Changes in ice front position on Greenland's outlet glaciers from 1992 to 2007, J. Geophys. Res.-Earth, 113, F02022, doi:10.1029/2007JF000927, 2008. 3091

Nesje, A.: Briksdalsbreen in western Norway: AD 1900–2004 frontal fluctuations as a combined effect of variations in winter precipitation and summer temperature, Holocene, 15, 1245–1252, 2005. 3088

Nesje, A., Lie, Ø., and Dahl, S. O.: Is the North Atlantic Oscillation reflected in Scandinavian glacier mass balance records?, J. Quaternary Sci., 15, 587–601, 2000. 3090

Nesje, A., Bakke, J., Dahl, S. O., Lie, Ø., and Matthews, J. A.: Norwegian mountain glaciers in the past, present and future, Global Planet. Change, 60, 10–27, 2008. 3073, 3088

Nuth, C., Kohler, J., König, M., von Deschwanden, A., Hagen, J. O., Kääb, A., Moholdt, G., and Pettersson, R.: Decadal changes from a multi-temporal glacier inventory of Svalbard, The Cryosphere, 7, 1603–1621, doi:10.5194/tc-7-1603-2013, 2013. 3071, 3073, 3084, 3091

Oerlemans, J. and Reichert, B. K.: Relating glacier mass balance to meteorological data by using a seasonal sensitivity characteristic, J. Glaciol., 46, 1–6, 2000. 3088, 3089

Østrem, G. and Haakensen, N.: Glaciers of Norway, in: Satellite image atlas of glaciers of the world, edited by: Williams, R. S. and Ferrigno, J. G., US Geological Survey, Professional Paper, 1386-E-3, 53 pp., 1993. 3079, 3087

Østrem, G. and Ziegler, T.: Atlas over breer i Sør-Norge (Atlas of glaciers in South Norway), Hydrologisk avdeling, Norges Vassdrags- og Elektrisitetsvesen, Meddelelse, Oslo, Norway, 20, 207 pp., 1969. 3071, 3073, 3080

Østrem, G., Haakensen, N., and Melander, O.: Atlas over breer i Nord-Skandinavia (Glacier atlas of Northern Scandinavia), Hydrologisk avdeling, Norges Vassdrags- og Energiverk, Meddelelse, Oslo, Norway, 22, 315 pp., 1973. 3071, 3073, 3080

Østrem, G., Selvig, K. D., and Tandberg, K.: Atlas over breer i Sør-Norge (Atlas of glaciers in South Norway), Hydrologisk avdeling, Norges Vassdrags- og Energiverk, Meddelelse, Oslo, Norway, 61, 180 pp., 1988. 3071, 3073, 3080

Paul, F. and Andreassen, L. M.: A new glacier inventory for the Svartisen region, Norway, from Landsat ETM+ data: challenges and change assessment, J. Glaciol., 55, 607–618, 2009. 3071, 3076

Paul, F., and Kääb, A.: Perspectives on the production of a glacier inventory from multispectral satellite data in Arctic Canada: Cumberland Peninsula, Baffin Island, Ann. Glaciol., 42, 59–66, 2005. 3071, 3076

Paul, F., Kaab, A., Maisch, M., Kellenberger, T., and Haeberli, W.: The new remote-sensing-derived Swiss glacier inventory: I. Methods, Ann. Glaciol., 34, 355–361, 2002. 3071, 3076
Paul, F., Huggel, C., Kääb., A., and Kellenberger., T.: Comparison of TM-derived glacier areas with higher resolution data sets, EARSeL eProceedings, 2, 15–21, CD-ROM, 2003. 3076
Paul, F., Kääb, A., Maisch, M., Kellenberger, T., and Haeberli, W.: Rapid disintegration of Alpine glaciers observed with satellite data, Geophys. Res. Lett., 31, L21402, doi:10.1029/2004GL020816, 2004. 3087
Paul, F., Kääb, A., and Haeberli, W.: Recent glacier changes in the Alps observed by satellite: consequences for future monitoring strategies, Global Planet. Change, 56, 111–122, 2007. 3071, 3089
Paul, F., Barry, R., Cogley, J. G., Frey, H., Haeberli, W., Ohmura, A., Ommanney, C. S. L., Raup, B., Rivera, A., and Zemp, M.: Recommendations for the compilation of glacier inventory data from digital sources, Ann. Glaciol., 50, 119–126, 2009. 3081
Paul, F., Andreassen, L. M., and Winsvold, S. H.: A new glacier inventory for the Jostedalsbreen region, Norway, from Landsat TM scenes of 2006 and changes since 1966, Ann. Glaciol., 52, 153–162, 2011. 3071, 3080, 3082, 3086
Paul, F., Barrand, N. E., Baumann, S., Berthier, E., Bolch, T., Casey, K., Frey, H., Joshi, S. P., Konovalov, V., Bris, R. L., Molg, N., Nosenko, G., Nuth, C., Pope, A., Racoviteanu, A., Rastner, P., Raup, B., Scharrer, K., Steffen, S., and Winsvold, S.: On the accuracy of glacier outlines derived from remote-sensing data, Ann. Glaciol., 54, 171–182, 2013. 3076, 3077
Racoviteanu, A. E., Paul, F., Raup, B., Khalsa, S. J. S., and Armstrong, R.: Challenges and recommendations in mapping of glacier parameters from space: results of the 2008 Global Land Ice Measurements from Space (GLIMS) workshop, Boulder, Colorado, USA, Ann. Glaciol., 50, 53–69, 2010. 3071
Radić, V., and Hock, R.: Glaciers in the Earth's hydrological cycle: assessments of glacier mass and runoff changes on global and regional scales, Surv. Geophys., 35, 813–837, doi:10.1007/s10712-013-9262-y, 2013. 3071
Rasmussen, L.: Spatial extent of influence on glacier mass balance of North Atlantic circulation indices, Terra Glacialis, 11, 43–58, 2007. 3090
Raup, B., Khalsa, S. J. S., Armstrong, R., and Racoviteanu, A.: The GLIMS Glacier Database: Status and Summary Analysis, MOCA09 – Our Warming Planet, IAMAS, IAPSO and IACS 2009 Joint Assembly, 2009. 3084, 3091

Sidjak, R. W. and Wheate, R. D.: Glacier mapping of the Illecillewaet icefield, British Columbia, Canada, using Landsat TM and digital elevation data, Int. J. Remote Sens., 20, 273–284, 1999. 3071

Winkler, S., Elvehøy, H., and Nesje, A.: Glacier fluctuations of Jostedalsbreen, western Norway, during the past 20 years: the sensitive response of maritime mountain glaciers, Holocene, 19, 395–414, 2009. 3086, 3088

Discussion Paper | Discussion Paper | Discussion Paper | Discussion Paper |

TCD

8, 3069–3115, 2014

Glacier area and length changes in Norway

S. H. Winsvold et al.

Table 1. The maximum, minimum and mean time span in years within each epoch.

	Maximum time span	Minimum time span	Mean time span
Full epoch	54	14	32
Epoch 1	41	3	17
Epoch 2	18	6	12

Table 2. Landsat satellite images for the GI_{1990} and GI_{2000} inventories. The first 9 rows are images used in GI_{1990}, and the next 10 are used in GI_{2000}. Dovre, Jotunheimen and Hardangerjøkulen subregions were the first sites processed and did not include the TM_1 (e.g. Andreassen et al., 2008). (L1G = Image is from the Global Land Cover Facility (GLCF), L1T = Standard terrain correction, NVE = Norwegian Water Resources and Energy Directorate, CGEO = The center for GIS and Earth Observation, ESA (Kiruna) = European Space Agency (Kiruna ground station), USGS = US Geological Survey).

Area code	Region	Path/Row	Date	Sensor	Source	$\frac{TM_3}{TM_5}$[a]	TM_1[a]
$1a_{1990}$	Seiland	p197r10	8 Sep 1990	L5/TM	USGS – NVE	2.8	60
$1b_{1990}$	Øksfjord (Lyngen)	p196r11	3 Sep 1988	L4/TM	USGS – NVE	2.8	70
2_{1990}	Lyngen	p197r11	25 Aug 1988	L4/TM	USGS – L1T	2	60
3_{1990}	Frostisen	p197r11	25 Aug 1988	L4/TM	USGS – L1T	1.8	60
4_{1990}	Svartisen[b]	p199r13	15 Aug 1988	L5/TM	ESA (Kiruna) – NVE	2.6	60
5_{1990}	Okstind	p199r14	31 Aug 1988	L5/TM	USGS – L1T	2	60
6_{1990}	Dovre	p199r16	8 Sep 1988	L4/TM	USGS – NVE	1.8	60
7_{1990}	Jotunheimen	p200r17	15 Aug 1997	L5/TM	USGS – NVE	2.8	35
9_{1990}	Hardanger/Folgefonna	p200r18	6 Aug 1988	L5/TM	USGS – NVE	2.4	60
1_{2000}	Seiland/Øksfjord	p196r11/10	28 Aug 2006	L5/TM	USGS – NVE	2.4	35
2_{2000}	Lyngen	p198r11	20 Aug 2001	L7/ETM+	USGS – CGEO	2.4	60
3_{2000}	Frostisen	p198r12	20 Aug 2001	L7/ETM+	USGS – L1G	2.6	60
4_{2000}	Svartisen	p199r13	7 Sep 1999	L7/ETM+	USGS – CGEO	2.6	59
5_{2000}	Okstindbreen	p199r14	7 Sep 1999	L7/ETM+	USGS – L1G	2.6	60
6_{2000}	Dovre	p199r16	9 Aug 2003	L5/TM	USGS – CGEO	2	–
7_{2000}	Jotunheimen	p199r17	9 Aug 2003	L5/TM	USGS – CGEO	2	–
8_{2000}	Hardangerjøkulen	p199r18	9 Aug 2003	L5/TM	USGS – CGEO	2	–
9_{2000}	Jostedalsbreen	p201r17/16	16 Sep 2006	L5/TM	USGS – NVE	2	35
10_{2000}	Folgefonna	p201r18	13 Sep 2002	L7/ETM+	USGS – NVE	2	35

[a] Values are larger than or equal to the given treshold.
[b] The Blåmannsisen subregion used the threshold values $\frac{TM_3}{TM_5} \geq 1.6$ and $TM_1 \geq 35$ due to cirrus clouds.

TCD
8, 3069–3115, 2014

Glacier area and length changes in Norway

S. H. Winsvold et al.

TCD
8, 3069–3115, 2014

Glacier area and length changes in Norway

S. H. Winsvold et al.

Table 3. Glacier area change (GAC) for three parts of Norway, and the change in the overall glaciated area for the three epochs. $\overline{\text{GAC}(\text{km}^2)}$ represent the average change for all glacier units included in the analysis.

	Full epoch			Epoch 1			Epoch 2		
	km^2	%	$\overline{GAC(km^2)}$	km^2	%	$\overline{GAC(km^2)}$	km^2	%	$\overline{GAC(km^2)}$
North	−76.4	−16.5	−0.116	−87.4	−19.5	−0.141	17.7	4.7	0.023
Central	−31.8	−4.0	−0.048	−83.2	−10.8	−0.145	56.9	8.3	0.092
South	−218.0	−12.6	−0.156	−18.8	−3.2	−0.038	−41.8	−7.1	−0.073
Norway	−326.1	−10.9	−0.12	−189.4	−10.5	−0.112	32.9	2.0	0.017
Norway a^{-1}	−10.5	−0.4	−0.004	−11.8	−0.7	−0.009	2.7	0.2	0.001

Table 4. Glacier length change (GLC) for three parts of Norway, and the change in the overall glaciated area for the three epochs. $\overline{\mathrm{GLC}}$(m) represent the average change for all glacier units included in the analysis.

	Full epoch	Epoch 1	Epoch 2
	GLC(m)	GLC(m)	GLC(m)
North	−357	−254	−82
Central	−204	−221	−22
South	−221	−129	−68
Norway	−241	−199	−55
Norway a^{-1}	−8	−14	−5

TCD
8, 3069–3115, 2014

Glacier area and length changes in Norway

S. H. Winsvold et al.

Table 5. Glacier length changes vs. in situ length changes. Engabreen is the only glacier with comparable data from northern Norway. The IDs refer to the glacier IDs in Andreassen et al. (2012b). For Midtdalsbreen (ID 2964) the measurements started in 1982, which means only epoch 2 was compared with in situ measurements for this glacier. Rembedalskåka (ID 2968) has discontinuous registrations in epoch 1 and 2. Five outlet glaciers from Jostedalsbreen (IDs: 2289, 2297, 2316, 2327, 2480) were not mapped in the GI_{1990} data set, and for these glaciers length changes are only calculated for the full epoch. FE = Full epoch, E1 = Epoch 1 and E2 = Epoch 2. Na = Not Available.

	In situ (m)			Maps/satellite (m)			Deviation (m)					
Name (GlacierID)	FE	E1	E2	FE	E1	E2	FE	E1	E2	Pix.[a]	Start[b]	Period[c]
Engabreen (1094)	149	19	130	256	147	109	107	128	21	4	1969	1968–1999
Fåbergstålsbreen (2289)	−950	Na	Na	−624	Na	Na	326	Na	Na	11	1967	1966–2006
Nigardsbreen (2297)	−268	Na	Na	−235	Na	Na	33	Na	Na	1	1972	1966–2006
Briksdalsbreen (2316)	25	Na	Na	44	Na	Na	19	Na	Na	1	1967	1966–2006
Austerdalsbreen (2327)	−197	Na	Na	−229	Na	Na	−32	Na	Na	−1	1967	1966–2006
Stigaholtbreen (2480)	−705	Na	Na	−369	Na	Na	336	Na	Na	11	1967	1966–2006
Storbreen (2636)	−60	−22	−38	−80	−18	−62	−20	4	24	−1	1984	1981–2003
Leirbreen (2638)	−146	−92	−54	−143	−65	−78	3	27	24	0	1982	1981–2003
Styggedalsbreen (2680)	−78	−64	−14	−66	−54	−12	12	10	−2	0	1982	1981–2003
Hellstugubreen (2786)	−269	−222	−47	−228	−171	−57	41	51	10	1	1983	1981–2003
Midtdalsbreen (2964)	Na	Na	−3	−200	−150	−50	Na	Na	47	Na	1989	1988–2003
Rembedalskåka (2968)	−55	Na	Na	−8	Na	Na	47	Na	Na	2	1977	1973–2003

[a] Number of pixels that differs between the ground measured and remotely sensed measurements for the full epoch. The spatial resolution of the sensor pixel is 30 m.
[b] Start year of the in situ data series, as close as possible to the start of the full epoch (topographic maps).
[c] The years compared for the full epoch.

TCD
8, 3069–3115, 2014

Table 6. Mean decadal area and length change from the beginning of the 1900s to the 2000s for five ice caps, divided into four epochs. We refer to the change between GI_{1900} and GI_{n50} as epoch 0. The whole period refer to the glacier change between GI_{1900} and GI_{2000}.

	Epoch 0	Epoch 1	Epoch2	Whole period
Decadal area change (km^2)	−0.13	−0.04	−0.03	−0.19
Decadal length change (m)	−73	−35	−42	−158

Table 7. Change assessment for West-Finnmark. Mean glacier change within the whole period (GI_{1900} and GI_{2000}). Decadal mean change and percentage total change.

Glacier	Sample		Mean change		Mean decadal change		Total change (%)	
	$A(n)$	$L(n)$	A(km^2)	L(m)	A(km^2)	L(m)	Area	Length
Nordmannsjøkelen (N)	9	1	−2.27	−1470	−0.32	−210	−91	−51
Seilandsjøkelen (Se)	6	4	−4.16	−1597	−0.59	−228	−71	−50
Langfjordjøkelen (L)	12	6	−0.95	−1231	−0.14	−187	−62	−43
Svartfjelljøkelen (Sv)	13	3	−0.34	−893	−0.05	−135	−46	−40
Øksfjordjøkelen (Ø)	17	12	−0.62	−795	−0.09	−120	−21	−27
All glaciers	57	26	−1.3	−1063	−0.19	−158	−53	−37

TCD
8, 3069–3115, 2014

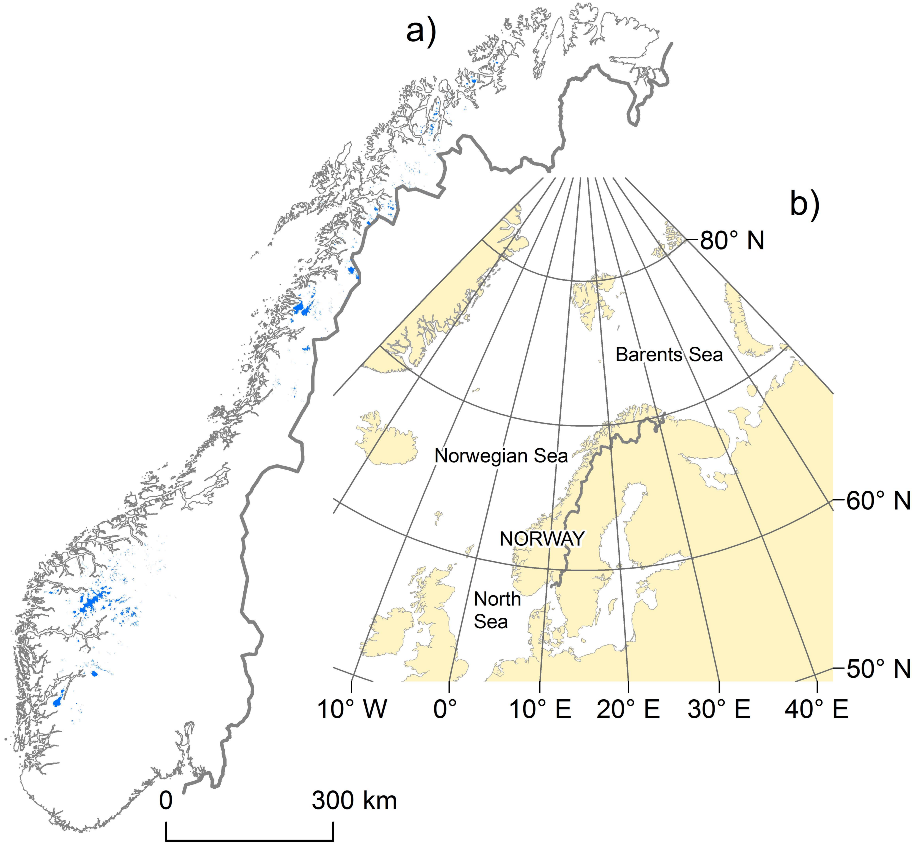

Figure 1. (a) The study area with Norwegian glaciers shown in blue, **(b)** Norway is bordering to the Norwegian sea in the west.

TCD
8, 3069–3115, 2014

Glacier area and length changes in Norway

S. H. Winsvold et al.

TCD
8, 3069–3115, 2014

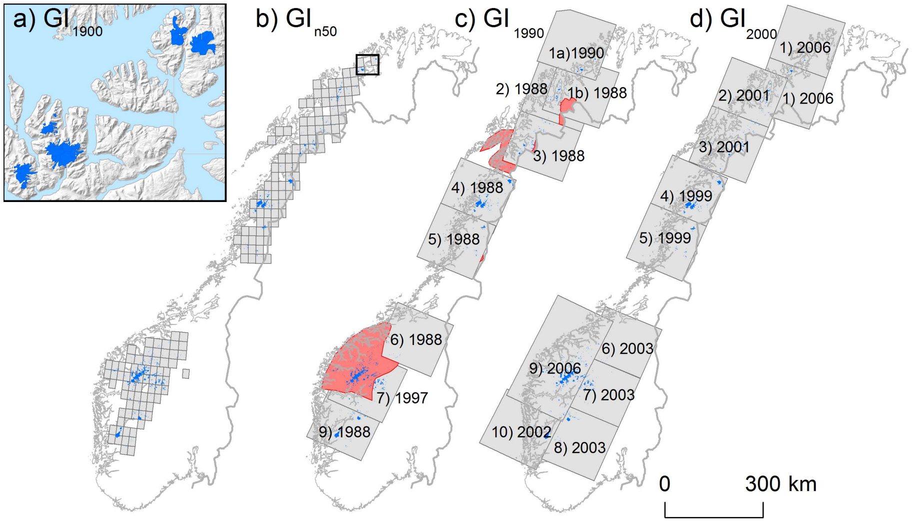

Figure 2. Spatial representation of the data sets, **(a)** A subset of five ice caps in northern Norway conducted in the period 1895–1907 (GI_{1900}), **(b)** GI_{n50} consists of 168 N50-map sheets based on aerial photographs within 1947–1985, **(c)** GI_{1990} consists of 9 Landsat TM4 and TM5 satellite scenes within 1988–1997. Red color shows where glaciers are not covered by suitable scenes, and **(d)** GI_{2000} includes 12 Landsat TM 5 and ETM+ 7 satellite scenes within 1999–2006.

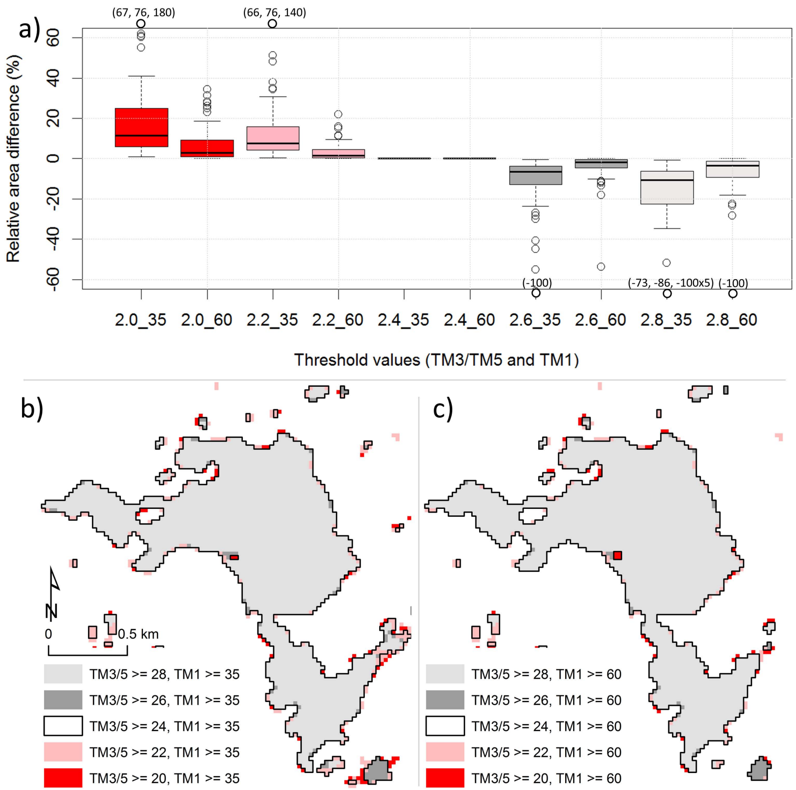

Figure 3. (a) Boxplot showing the relative area difference (%) for selected threshold values. The numbers in parentheses are outliers, **(b)** Visual representation of the threshold sensitivity for Nordmannsjøkelen. The threshold sensitivity is represented with increments of 0.2, using $\frac{TM_3}{TM_5} \geq 2.4$ and $TM_1 \geq 35$ as the initial threshold value (black line), and in **(c)** $\frac{TM_3}{TM_5} \geq 2.4$ and $TM_1 \geq 60$ are used for the initial threshold value. Some of the smallest glaciers or possible snow fields, are completely vanishing when the threshold values are increased.

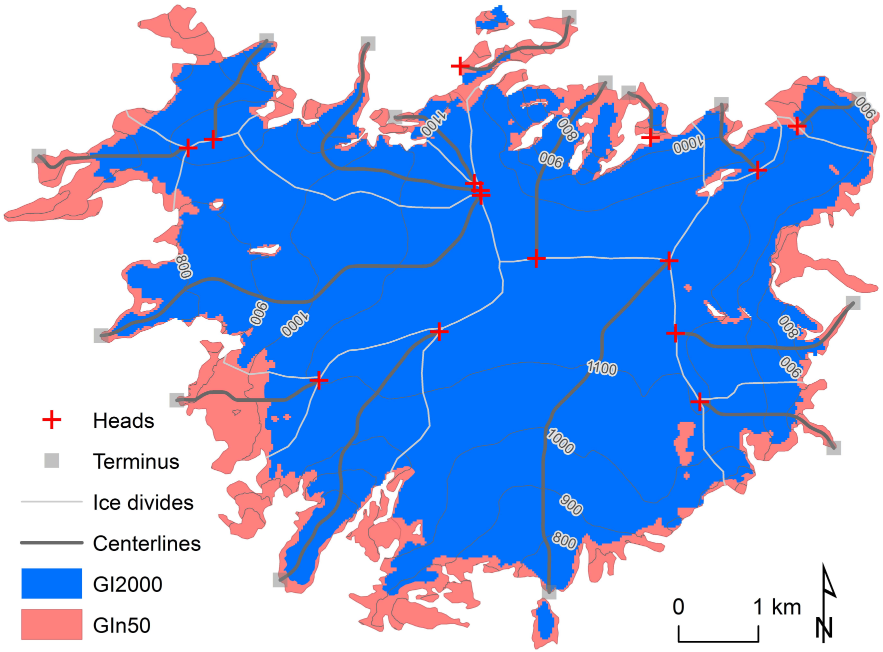

Figure 4. GI_{n50} and GI_{2000} presented with the automatic derived glacier heads, terminus and centerlines at Øksfjordjøkelen.

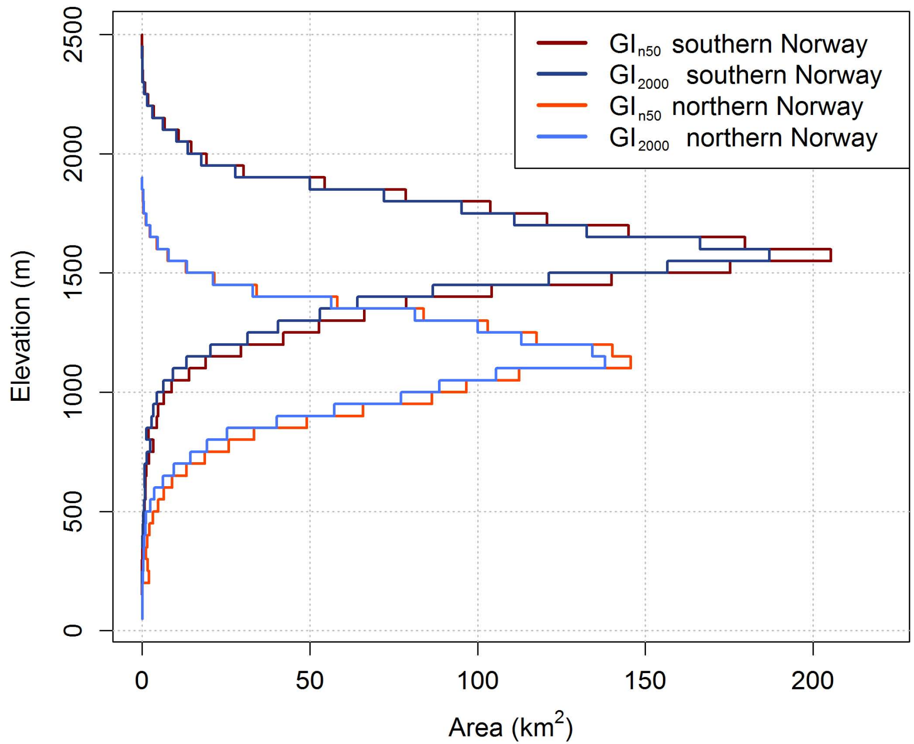

Figure 5. Distribution of glacier area with elevation for GI_{n50} and GI_{2000} for all glaciers in Norway. We only compare glaciers present in both data sets. The clear bi-modal distribution with a distinction between 1000–1350 m and 1400–1700 m illustrates the predominant location of glaciers in northern and southern Norway, respectively (Andreassen et al., 2012b). Note that northern Norway include the central and northern part presented in Figs. 6 and 7.

TCD
8, 3069–3115, 2014

Glacier area and length changes in Norway

S. H. Winsvold et al.

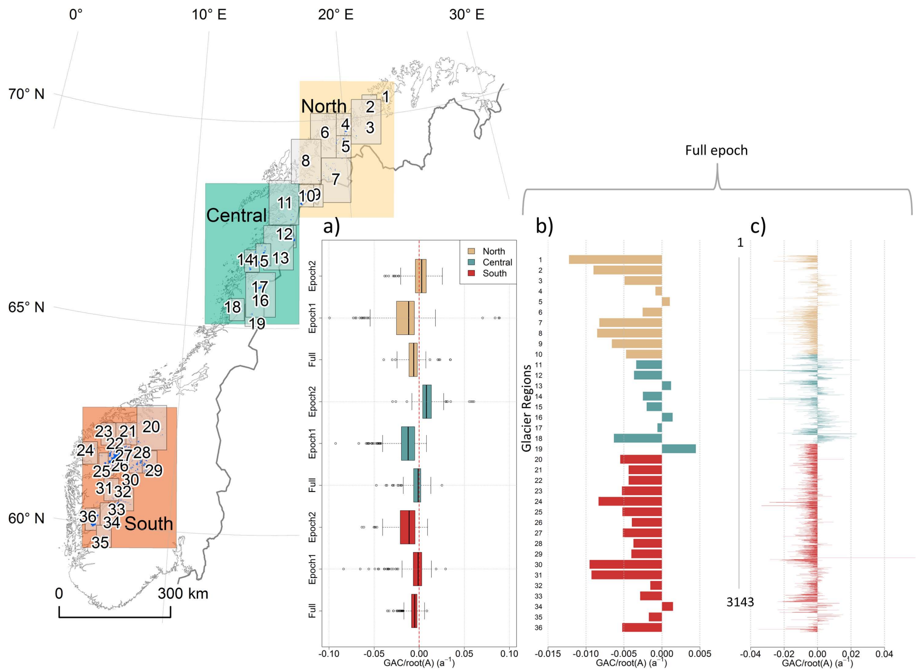

Figure 6. Glacier area change (GAC) ranging from north to south displayed for Norway, 36 glacier regions **(b)** and 1–3143 glacier units **(c)**. GAC is presented in $\frac{\text{GAC}}{\text{root}(A)}$ (see Sect. 4.5). **(a)** Boxplot showing the annual $\frac{\text{GAC}}{\text{root}(A)}$ for three parts in Norway, and for three epochs, **(b)** mean annual $\frac{\text{GAC}}{\text{root}(A)}$ for 36 glacier regions for the full epoch, and **(c)** $\frac{\text{GAC}}{\text{root}(A)}$ for each glacier unit for the full epoch. Glacier regions and glacier units are arranged in a north-south order as defined in Andreassen et al. (2012b). Only glaciers > 0.5 km^2 are included in **(a)**.

TCD

8, 3069–3115, 2014

Glacier area and length changes in Norway

S. H. Winsvold et al.

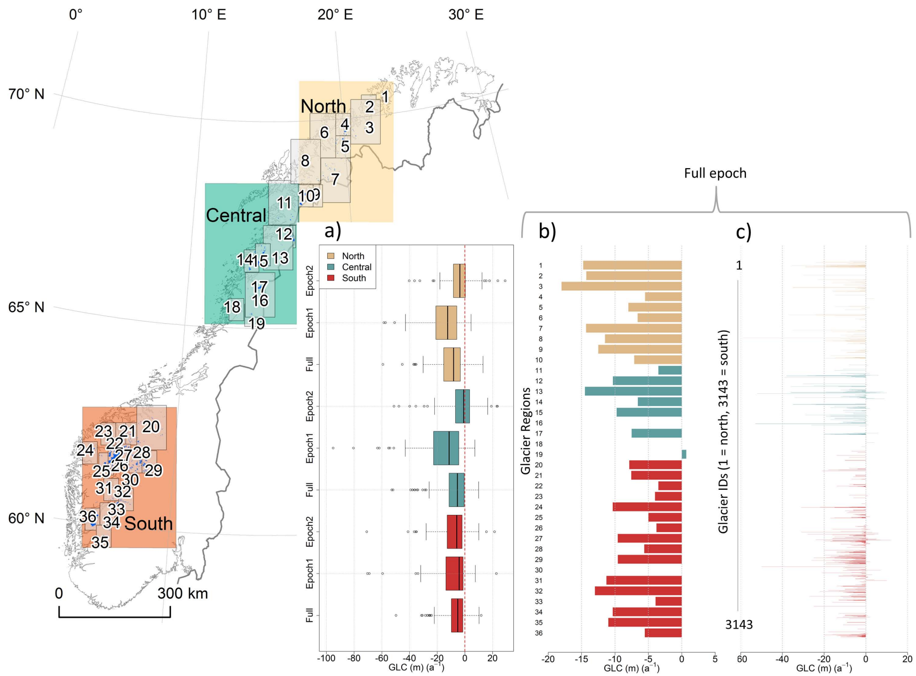

Figure 7. Glacier length change (GLC) ranging from north to south displayed for Norway, 36 glacier regions **(b)** and 1–3143 glacier units **(c)**. **(a)** Boxplot showing the annual GLC (m) for three parts of Norway, and for three epochs, **(b)** mean annual GLC (m) for 36 glacier regions for the full epoch. Note that glacier regions 16, 18 and 30 do not include any glacier length data, and **(c)** GLC (m) for each glacier unit for the full epoch. Glacier regions and the glacier units are arranged in a north-south order as defined in Andreassen et al. (2012b).

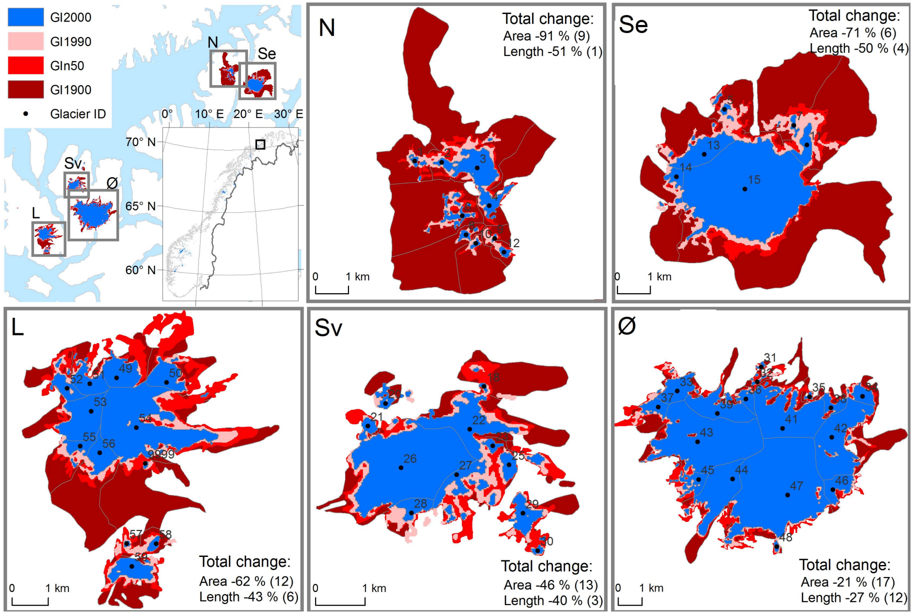

Figure 8. Glacier area and length change for five ice caps in West-Finnmark. The numbers after the mean percentage area and length change are the number of included glacier units (area) or centerlines (length). N = Nordmannsjøkelen, Se = Seilandsjøkelen, L = Langfjordjøkelen, Sv = Svartfjelljøkelen and Ø = Øksfjordjøkelen.

TCD

8, 3069–3115, 2014

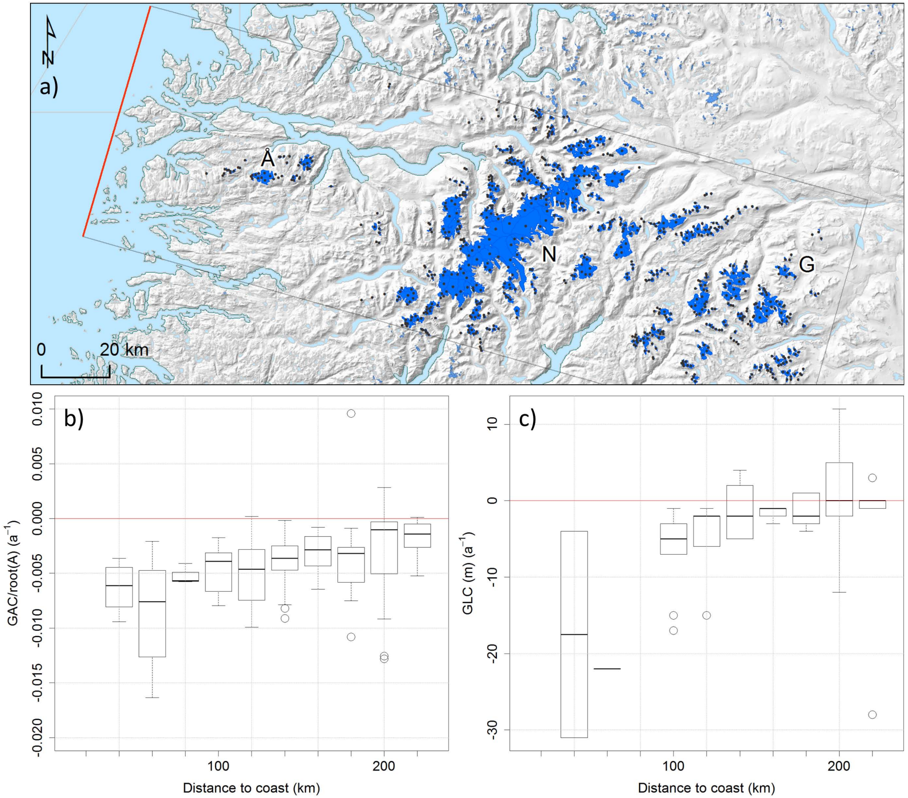

Figure 9. (a) Map of the west–east transect of glaciers in southern Norway, Å = Ålfotbreen, N = Nigardsbreen and G = Gråsubreen. Mean glacier change every 20 km from the coast for the full epoch is presented in boxplots for yearly glacier area change (units of length $\frac{\text{GAC}}{\text{root}(A)}$) in **(b)** and glacier length change (m) in **(c)**. All glaciers are included for GAC, and glaciers > 1 km^2 are included for GLC.

TCD
8, 3069–3115, 2014

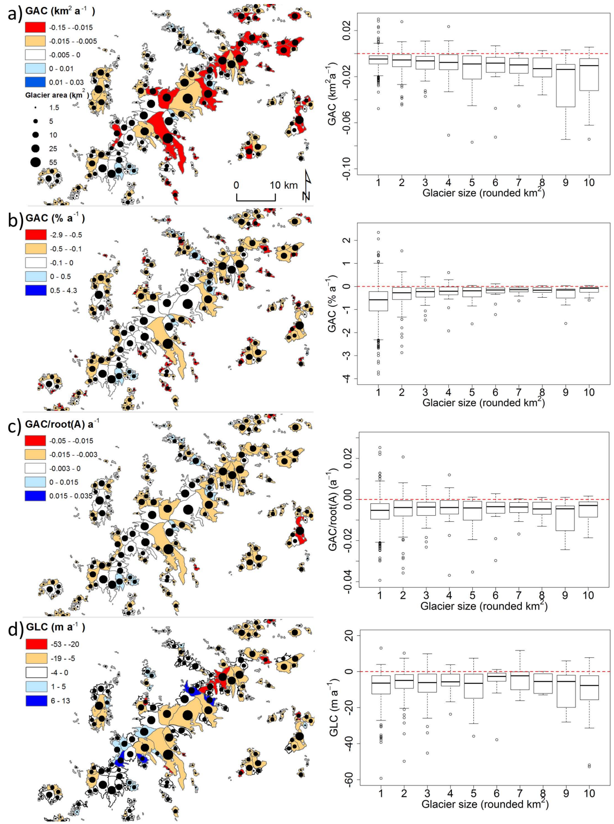

Figure 10. Glacier area change (GAC) and glacier length change (GLC) represented for the Jostedalsbreen region in western Norway. **(a)** GAC ($km^2\,a^{-1}$), **(b)** GAC ($\%\,a^{-1}$), **(c)** $\frac{GAC}{root(A)}\,a^{-1}$, and **(d)** GLC ($m\,a^{-1}$). The corresponding box plots includes all glaciers in Norway $> 0.5\,km^2$. Extreme values of **(a)** and **(b)** are enhanced in the map legend, to mark the point of problematic influence of glacier geometry and size when GAC is represented in km^2 and %.